

# Model for post-yield tension stiffening and rebar rupture in concrete members

Seong-Cheol Lee<sup>a</sup>, Jae-Yeol Cho<sup>b</sup>, Frank J. Vecchio<sup>a,\*</sup>

<sup>a</sup> The Department of Civil Engineering at University of Toronto, ON, Canada

<sup>b</sup> The Department of Civil and Environmental Engineering at Seoul National University, Seoul, Republic of Korea

## ARTICLE INFO

### Article history:

Received 25 February 2010

Received in revised form

6 January 2011

Accepted 9 February 2011

Available online 12 March 2011

### Keywords:

Tension stiffening

Crack

Bond

Post-yield

Ductility

Rupture

Reinforcement

## ABSTRACT

A tension stiffening model is presented which enables the calculation of average tensile stresses in concrete, after yielding of reinforcement, in reinforced concrete elements subjected to uniaxial tension, shear or flexure. To determine the average tensile stress–strain relationship for concrete, a crack analysis approach is employed taking into account the bond mechanism between concrete and deformed reinforcing bars, and numerical analyses are conducted to determine the tensile behavior of reinforced concrete members including post-yield response. Analytical parametric studies are conducted to determine the influence of various parameters including concrete compressive strength and reinforcement yield strength, ultimate strength, hardening stress, and hardening strain. Analysis results obtained from the proposed model, when compared to experimental results for uniaxial members, indicate good agreement for structural behavior after yielding of reinforcement. The proposed model makes it possible to accurately calculate reinforcement stresses at crack locations and, thus, average strain conditions which result in rupture of reinforcement. This leads to more realistic predictions of the uniaxial, flexural, and shear ductility of reinforced concrete members.

Crown Copyright © 2011 Published by Elsevier Ltd. All rights reserved.

## 1. Introduction

In a reinforced concrete member that has suffered cracking, the contribution of average post-cracking tensile stresses in the concrete must be appropriately considered in order to accurately predict the structural behavior of the member. After the tensile stress capacity of the concrete is exceeded and the member cracks, the concrete tensile stress at a crack drops to zero as the tension softening response is exhausted, but the concrete between cracks still attracts tensile stresses due to the effects of bond between the concrete and the reinforcing steel; this mechanism is known as tension stiffening. One approach to considering tension stiffening effects in the tensile behavior of concrete members is to formulate an average tensile stress–strain relationship for the concrete; this approach has been successfully used in finite element analysis [1] and sectional analysis [2] of concrete structures.

A variety of tension stiffening models have been developed for evaluating the average tensile stress of concrete [3–8]. Most have focused on the tensile behavior before yielding of reinforcement to predict the response illustrated with line *A–B* in Fig. 1 where *A* and *B* represent initial cracking of the concrete and yielding of the reinforcement at a crack, respectively. [In Fig. 1, the difference between the tensile stress in a concrete-embedded bar and that in a bare bar

is defined as the tension stiffening effect.] In addition, researchers recently investigated the effect of concrete shrinkage [9] and the bond–slip relationship [10] on the tension stiffening behavior, and presented an analytical procedure and a modified bond model, respectively.

In previous models [4–8], the equilibrium condition at a crack is typically checked using the yield strength of steel reinforcement as the limit capacity. After local yielding of the reinforcement at a crack, the average tensile stress of concrete due to tension stiffening is reduced because the total strength capacity across the crack is assumed to not exceed the yield strength of the reinforcement (line *B–C* in Fig. 1 where *C* denotes the point where the average tensile strain is equal to the yield strain of the reinforcement). (Unless this equilibrium check is performed, the capacity of the concrete member may be unconservatively evaluated due to an overestimation of concrete tensile stress.) Since local strains of the reinforcement in the vicinity of the crack abruptly increase without significant increase in the tension, points *B* and *C* in Fig. 1 do not coincide. With the crack equilibrium check imposed, after the average strain of the reinforcement reaches the yield strain, the average tensile stress of concrete becomes zero. Hence, once the average stress of the reinforcement has reached yield, the contribution of concrete on tensile behavior is typically ignored; the computed tensile behavior of a reinforced concrete member after yielding of reinforcement becomes the same as that of bare steel bars. Consequently, the customary equilibrium check at a crack results in the member's calculated

\* Corresponding author. Tel.: +1 416 978 5910; fax: +1 416 978 6813.

E-mail address: [fjv@civ.utoronto.ca](mailto:fjv@civ.utoronto.ca) (F.J. Vecchio).

**Nomenclature**

$a$	Coefficient for peak average concrete tensile stress after yielding of reinforcement
$A_c$	Tributary area of concrete for the steel reinforcement
$d_b$	Diameter of steel reinforcement
$E_c, E_s$	Young's modulus of concrete and steel reinforcement, respectively
$E_{sh}$	Hardening stress of steel reinforcement
$F_c, F_s$	Tensile forces due to concrete and steel reinforcement, respectively
$f_c, f_s$	Local tensile stresses of concrete and steel reinforcement, respectively
$f'_c, f_{cr}$	Concrete compressive strength and tensile strength, respectively
$f_{ct,avg}$	Average tensile stress of concrete
$f_{s1}$	Steel reinforcement stress over the length where $\epsilon_s = \epsilon_c$
$F_{scr}$	Tensile force due to steel reinforcement at crack
$f_{scr}$	Steel reinforcement tensile stress at crack
$f_{scr, \epsilon_t, peak}$	Steel reinforcement stress at crack when the average tensile strain of reinforced concrete is $\epsilon_{t, peak}$
$f_{scr, 0.1}$	Steel reinforcement stress at crack when average tensile strain of reinforced concrete is 0.1
$f_{s, avg}$	Average tensile stress of steel reinforcement
$f_{sr1}$	Steel reinforcement stress at crack when first crack has formed
$f_{srn}$	Steel reinforcement stress at crack when stabilized crack pattern has formed (last crack)
$f_{su}$	Rupture strength of steel reinforcement
$f_{sx}$	Steel reinforcement stress along the reinforcing bar
$f_{sy}$	Yield strength of steel reinforcement
$f_{ct, peak}$	Peak average tensile stress of concrete after yielding of reinforcement
$f_{ct, peak, \rho_{min}}$	$f_{ct, peak}$ With $\rho_{min}$
$K_b$	Bond coefficient taking into account the steel reinforcement strain
$l_t$	Transfer length
$n_E$	Modular ratio ( $=E_s/E_c$ )
$s_1$	Slip corresponding to the bond strength
$s_{cr}$	Crack spacing
$s_x$	Slip along the reinforcing bar
$s'$	Derivative of slip
$s'_0$	Derivative of slip at the section $x = 0$
$x$	Distance from the location at which $\epsilon_c = \epsilon_s$
$\alpha$	Power parameter in the bond stress–slip relationship
$\beta_t$	Coefficient to take into account the ratio $f_{sy}/f_{tu}$
$\epsilon_c, \epsilon_s$	Strains of concrete and steel reinforcement along the reinforcing bar, respectively
$\epsilon_{cr}$	Cracking strain of concrete ( $=f_{cr}/E_c$ )
$\epsilon_{scr}$	Steel strain at crack
$\epsilon_{sr1}$	Steel strain at the point of zero slip under cracking forces reaching concrete tensile strength
$\epsilon_{sr2}$	Steel strain at the crack under cracking forces reaching concrete tensile strength
$\epsilon_{sy}, \epsilon_{sh}, \epsilon_{su}$	Yield strain, hardening strain, and rupture strain of reinforcement, respectively
$\epsilon_{t, avg}$	Average tensile strain of reinforced concrete
$\epsilon_{t, avg, rup}$	Average tensile strain of reinforced concrete causing reinforcement rupture
$\epsilon_{t, peak}$	Average tensile strain of reinforced concrete at $f_{t, peak}$
$\rho_{min}$	Minimum reinforcement ratio
$\rho_s$	Reinforcement ratio
$\rho_v$	Stirrup ratio in reinforced concrete beam
$\tau_{b, x}$	Bond stress along the reinforcing bar
$\tau_{max}$	Bond strength

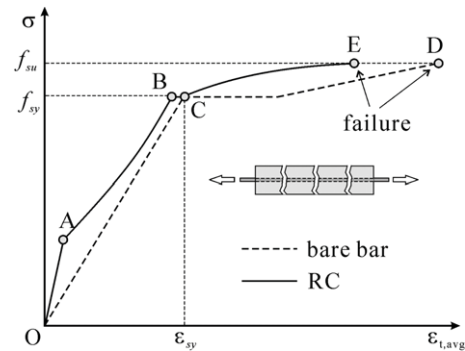


Fig. 1. Behavior of reinforced concrete members subjected to uniaxial tension.

ultimate strength and strain being identical to those of the bare steel bar (line C–D in Fig. 1).

However, average tensile stresses in the concrete still exist even after yielding of the reinforcement because of bond interaction between the concrete and steel. In other words, after the average tensile strain reaches the yield strain of the reinforcement, the total resistance of RC remains stiffer than that of the bare bar. The contribution of concrete tensile stress after yielding of reinforcement makes the average tensile strain of reinforced concrete at the ultimate state less than that of the bare steel bar (line C–E in Fig. 1). This means that the ductility of RC members subjected to direct tension can be significantly overestimated without the consideration of the post-yield tension stiffening behavior; it follows that the tension stiffening effect after yielding of reinforcement can be significant in the evaluation of the tensile, flexural or shear ductility of reinforced concrete members. Therefore, the tensile stress of concrete after yielding of reinforcement should be considered for more realistic calculations of the structural behavior of concrete members and structures.

**2. Research significance**

Although a number of tension stiffening models have been proposed, most have focused on the tensile behavior before yielding of reinforcement. They typically assume that no tension stiffening effects prevail after yielding of the reinforcement and, consequently, they will over-estimate a structure's deformation capacity. The tension stiffening model proposed in this study, which considers the average tensile stress of concrete after yielding of reinforcement, will enable more realistic predictions of the tensile, flexural, or shear behavior of reinforced concrete members, including better representations of post-yielding stiffness, strength and ductility. This is significant for applications requiring accurate performance assessment of structures. As well, it will enable improved estimates of strength and deformation capacity in concrete elements reinforced with nonductile reinforcement such as glass or carbon FRP bars.

**3. Analysis of RC members subjected to uniaxial tension**

The crack analysis procedure presented by Balázs [11] is used, in this paper, to evaluate average concrete tensile stresses in members subjected to uniaxial tension. In this section, the crack analysis procedure is summarized with particular consideration given to yielding of reinforcement. Analysis results thus obtained are compared with existing tension stiffening models and experimental results. The procedure is later employed to develop a tension stiffening model for post-yield behavior.

**3.1. Local bond behavior of RC members subjected to uniaxial tension**

In respect to the bond slip–stress relationship between concrete and reinforcement steel, analysis procedures for the tensile

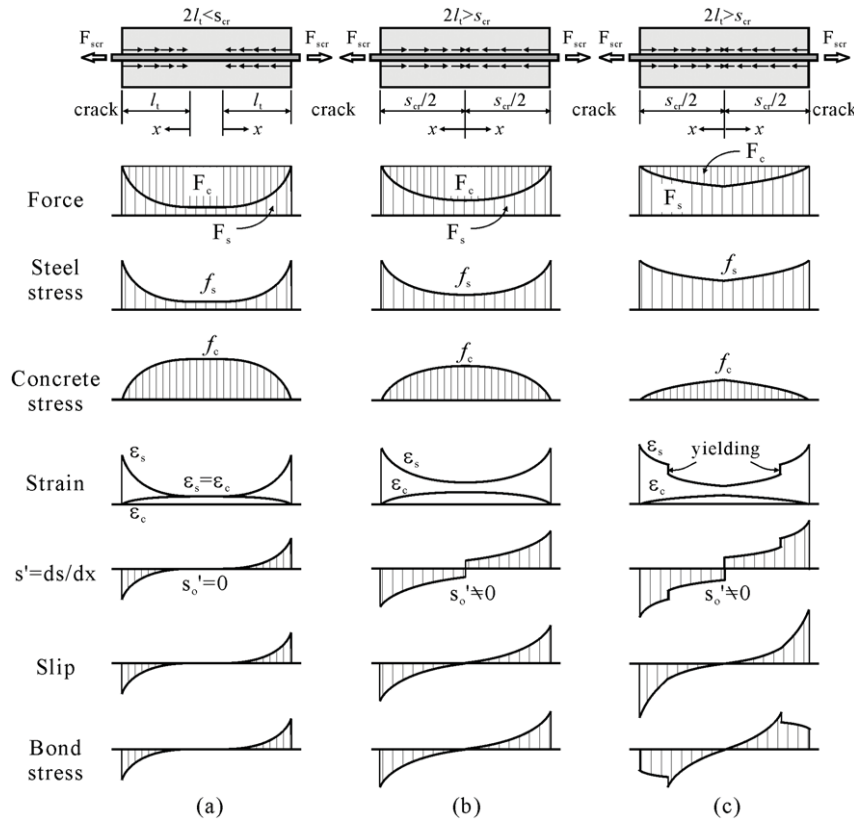


Fig. 2. Force, stress, strain, slip, and bond stress distribution between cracks; (a) initial crack formation; (b) stabilized crack before yielding; (c) stabilized crack after yielding.

behavior of concrete members subjected to uniaxial tension have been presented by several researchers (e.g., [11,12]). In these crack analysis models, the crack width can be obtained from the slip, which is calculated by integration of the difference between concrete and reinforcing steel strains. The integration should be conducted over the entire transfer length; that is, half the crack spacing.

The post-cracking behavior of reinforced concrete members can be divided into two stages; the initial crack formation stage and the stabilized crack stage. The stabilized crack stage, in turn, can be sub-divided into responses before and after yielding of reinforcement.

Distributions of the steel and concrete stresses, strains, and bond stresses, between the cracks, are illustrated in Fig. 2. As shown in Fig. 2(a), the concrete stress at a crack is negligible and the reinforcement must carry the entire applied tensile load. Since the tensile stress is transferred from the reinforcement to the concrete due to bond mechanisms, the tensile stress of concrete increases with distance from the crack within the transfer length. Therefore, slip between steel and concrete develops within the transfer length, and is a maximum at the crack. With increasing tensile force, additional cracks can develop since the concrete stress between cracks may increase up to the concrete tensile strength.

With increasing load applied, the crack spacing becomes smaller than twice the transfer length as shown in Fig. 2(b). This state is denoted as the stabilized crack formation stage. Generally, in reinforced concrete members subjected to uniformly-distributed uniaxial tension, the crack development stabilizes after first cracking. With further increases in tension force, the reinforcement reaches its yield stress. At this stage, as shown in Fig. 2(c), steel stress exhibits a sudden change due to the yielding, and thus the derivative of slip is discontinuous at this location. Moreover, the bond efficiency is decreased with large tensile

straining of the steel; consequently, the bond stress gradually decreases after yielding of reinforcement.

### 3.2. Crack analysis procedure of RC members subjected to uniaxial tension

As noted by several researchers [11,12], the differential equation relating slip and bond stress can be expressed by the following equation:

$$s''_x - \frac{4(1 + n_E \rho_s)}{d_b E_s} \tau_{bx} = 0. \quad (1)$$

In the initial crack formation stage, the bond stress–slip relationship between concrete and steel reinforcement for relatively small slip has been described as follows [3]:

$$\tau_{bx} = \tau_{\max} \left( \frac{s_x}{s_1} \right)^\alpha. \quad (2)$$

With this bond stress–slip relationship, differential Eq. (1) can be solved as follows:

$$s_x = \left( \frac{2(1 - \alpha)^2 (1 + n_E \rho_s) \tau_{\max} x^2}{(1 + \alpha) E_s s_1^\alpha d_b} \right)^{1/(1-\alpha)}. \quad (3)$$

By substituting Eq. (3) into Eq. (2), the steel stress distribution is described by Eq. (4).

$$f_{sx} = f_{s1} + K \left( \frac{x^{1+\alpha}}{s_1^\alpha d_b} \right)^{1/(1-\alpha)} \quad (4)$$

where

$$K = \tau_{\max} \frac{4(1 - \alpha)}{1 + \alpha} \left( \frac{2(1 - \alpha)^2 (1 + n_E \rho_s) \tau_{\max}}{(1 + \alpha) E_s} \right)^{\alpha/(1-\alpha)}. \quad (5)$$

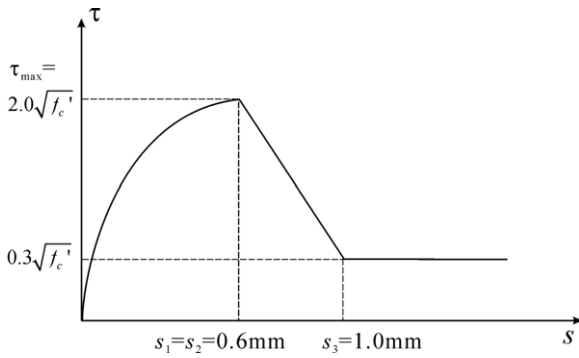


Fig. 3. Bond stress-slip relationship for unconfined concrete with good bond, CEB-FIP MC90 [3].

From Eqs. (4) and (5), the transfer length can be derived using known boundary conditions at the crack ( $f_{sx} = f_{scr}$  at  $x = l_t$ ); thus:

$$l_t = \left( \frac{(s_1^\alpha d_b)^{1/(1-\alpha)} f_{scr}}{1 + n_E \rho_s K} \right)^{(1-\alpha)/(1+\alpha)} \quad (6)$$

The crack width, which is twice the slip at the crack, can then be calculated:

$$w = 2 \left( \frac{s_1^\alpha d_b (1 + \alpha) f_{scr}^2}{8(1 + n_E \rho_s) \tau_{max} E_s} \right)^{1/(1+\alpha)} \quad (7)$$

Generally, in reinforced concrete members subjected to uniformly-distributed uniaxial tension, the crack spacing at the first cracking should be between  $l_t$  and  $2l_t$ . In this paper, the average crack spacing has been assumed as  $4l_t/3$  as suggested in CEB-FIP MC90 [3]. Since the transfer length increases with increasing steel stress at the crack as shown in Eq. (6), the cracking behavior of members subjected to uniformly-distributed uniaxial tension should follow the stabilized crack formation stage after the first cracking phase. For additional cracks with increasing tensile load, it can be assumed that a new crack will form midway between two adjacent cracks where the concrete stress is greatest. Unlike the analysis for the initial crack formation stage, an explicit mathematical solution for the stabilized cracking behavior is not possible. In this study, therefore, the fourth-order Runge-Kutta method, which is a numerical method applicable to second order differential equations, has been employed.

Since the slip between concrete and reinforcement generally increases with an increase in the applied tensile force, and varies along the reinforcement, the variation of the bond stress should be considered. In this paper, the bond stress-slip relationship [3] shown in Fig. 3 is assumed for unconfined concrete in good-bond condition. Adding to the effects of slip, a large tensile strain in the reinforcing bar causes a further reduction in the bond stress as shown in Fig. 2(c). To incorporate the influence of steel strain, the following bond coefficient [13], which is to be multiplied by the bond stress calculated from the basic bond stress-strain relationship, has been used:

$$K_b(\epsilon_s) = \exp[\min\{0, 10(\epsilon_{sy} - \epsilon_s)\}]. \quad (8)$$

The algorithm for the crack analysis procedure is presented in Fig. 4.

### 3.3. Comparison of existing tension stiffening models

A reinforced concrete member tested by Mayer and Eligehausen [14] was used for verification of the crack analysis procedure. The compressive cube strength of concrete was 28.4 MPa; the

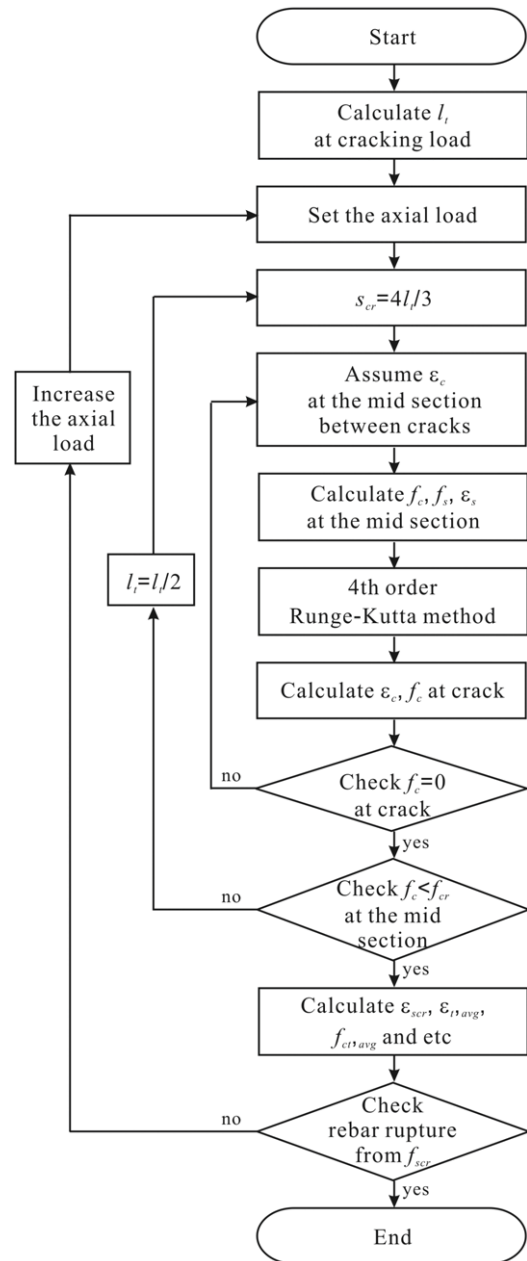


Fig. 4. Algorithm for the crack analysis procedure.

longitudinal reinforcement ratio was 0.5% and the diameter of reinforcement was 16 mm. In tensile tests of the bare steel bar, the reinforcement ruptured at an average tensile strain of 0.085. The same reinforcement, within the concrete tension member, ruptured at an average strain of 0.045, representing a 47% reduction. Accounting for the stiffening effects of concrete, the proposed formulation predicts an average rupture strain of 0.039, reasonably close to the observed value.

The uniaxial tensile stress-strain relationship obtained from the crack analysis procedure is compared to the experimental results in Fig. 5. It is noted that this analysis method was performed assuming increasing force-controlled loading. The predicted response is seen to agree reasonably well with the experimentally observed response, particularly in the post-yielding regime. Note that local strain hardening of the reinforcement across the cracks results in force capacities greater than the yield strength at relatively low levels of average strain.

**Table 1**  
Summary of tension stiffening models for cracked concrete.

Source	Tension stiffening model
CEB-FIP MC90 [3]	$\epsilon_{t,avg} = \epsilon_{scr} - \frac{\beta_t(f_{scr}-f_{sr1})+(f_{sm}-f_{scr})}{f_{sm}-f_{sr1}}(\epsilon_{sr2} - \epsilon_{sr1})$ for $f_{sr1} < f_{scr} \leq f_{sm}$ $\epsilon_{t,avg} = \epsilon_{scr} - \beta_t(\epsilon_{sr2} - \epsilon_{sr1})$ for $f_{sm} < f_{scr} \leq f_y$
Vecchio & Collins [4]	$\epsilon_{t,avg} = \epsilon_{sy} - \beta_t(\epsilon_{sr2} - \epsilon_{sr1}) + \delta \left(1 - \frac{f_{sr1}}{f_{yk}}\right)(\epsilon_{scr} - \epsilon_{sy})$ for $f_y < f_{s2} \leq f_{tu}$
Collins & Mitchell [5] Vecchio & Collins [6]	$f_{ct,avg} = \frac{f_{cr}}{1 + \sqrt{200\epsilon_{t,avg}}}$
Bentz [7]	$f_{ct,avg} = \frac{f_{cr}}{1 + \sqrt{500\epsilon_{t,avg}}}$
Stramandinoli & Rovere [8]	$f_{ct,avg} = \frac{f_{cr}}{1 + \sqrt{3.6M\epsilon_{t,avg}}}$ where, $M = \frac{A_c}{\sum d_b \pi}$ $f_{ct,avg} = f_{cr} \exp\left(-\alpha_t \frac{\epsilon_{t,avg}}{\epsilon_{cr}}\right)$ where, $\alpha_t = 0.017 + 0.255(n_E \rho_s) - 0.106(n_E \rho_s)^2 + 0.016(n_E \rho_s)^3$

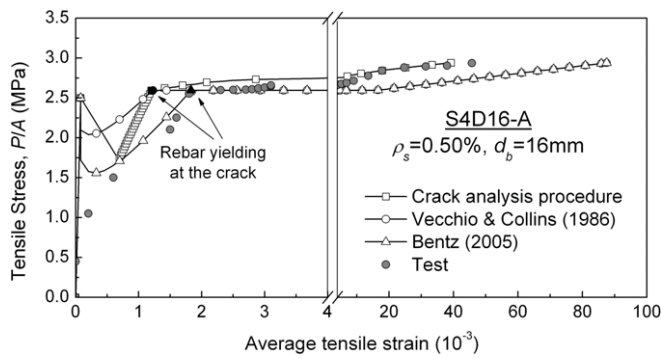


Fig. 5. Analysis results for reinforced concrete member subjected to tension.

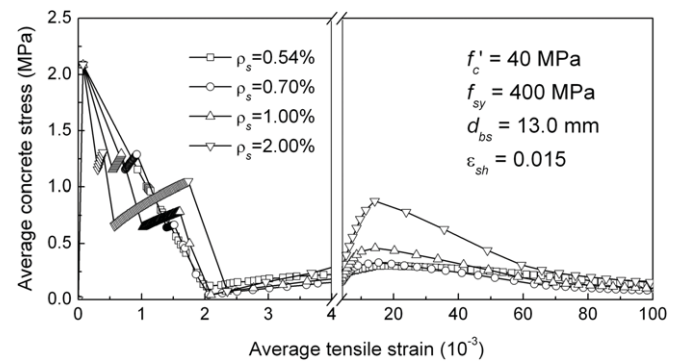


Fig. 7. Effect of reinforcement ratio on average tensile stress in concrete.

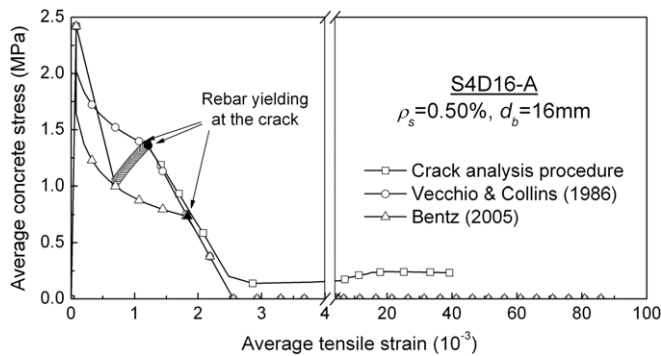


Fig. 6. Calculated average tensile stress in concrete.

The concrete average tensile stress, as calculated by the crack analysis procedure for this test specimen, was compared with values obtained from various tension stiffening models commonly used for the analysis of reinforced concrete structures. (See Table 1.) [It should be noted that the average tensile stress of concrete is calculated by subtracting the steel bare bar stress component from the total tensile force in the member.] As shown in Fig. 6, although there are some differences in the concrete average tensile stress prior to yielding of reinforcement at the crack, they are not significant; the crack analysis procedure based on the Balázs model [11] returns values between those obtained from the Vecchio and Collins [6] and Bentz [7] models. After yielding of reinforcement, however, the latter two models do not allow for tensile stress contributions from the concrete since the total strength capacity at a crack is limited by the yield strength and post-yield response of the reinforcement. Consequently, this assumption results in predictions where the ultimate tensile strain of a reinforced concrete member is the same as that of the bare steel bar. On the other hand, the contribution from concrete to the post-yielding tension response can be evaluated, reasonably accurately, by the crack analysis procedure described.

#### 4. Tension stiffening model after yielding of reinforcement

Using the crack analysis procedure described above, analytical parametric studies were undertaken to investigate factors which influence concrete average tensile stresses after yielding of reinforcement. A simplified post-yielding tension stiffening model was formulated accordingly.

##### 4.1. Analytical parametric study of uniaxial tensile behavior

The parameters considered in the parametric study were the concrete compressive strength (20, 40, 60, and 80 MPa) and the reinforcement yield strength (200, 300, 400, 500, and 600 MPa), hardening strain (yield strain, 0.01, 0.02, and 0.03), strain hardening modulus (500, 1000, 3000, and 5000 MPa), bar diameter (6, 10, 13, 16, 19, and 22 mm), and reinforcement ratio (0.5%, 0.7%, 1.0%, and 2.0%). The Young's modulus of reinforcement steel was fixed at 200,000 MPa. The tensile strength and Young's modulus of concrete were assumed to be  $f_{cr} = 0.33\sqrt{f'_c}$  and  $E_c = 3300\sqrt{f'_c} + 6900$  MPa [16], respectively.

Fig. 7 provides an example of typical results obtained from the analytical parametric study. The concrete average tensile stress initially increases after yielding of the reinforcement, peaks and then gradually diminishes. Although the peak post-yielding tensile stress in the concrete, and the corresponding strain, are significantly affected by the parameters considered, the overall behavior can be represented as shown in Fig. 8. In this figure, points A through E have the same meanings as the corresponding points in Fig. 1. The analytical parametric study undertaken focused on two aspects: the peak post-yielding tensile stress in the concrete, and the average tensile strain at peak stress.

##### 4.2. Peak average tensile stress in concrete after yielding of reinforcement

From the results of the parametric analysis, it was determined that the peak average tensile stress in concrete after yielding

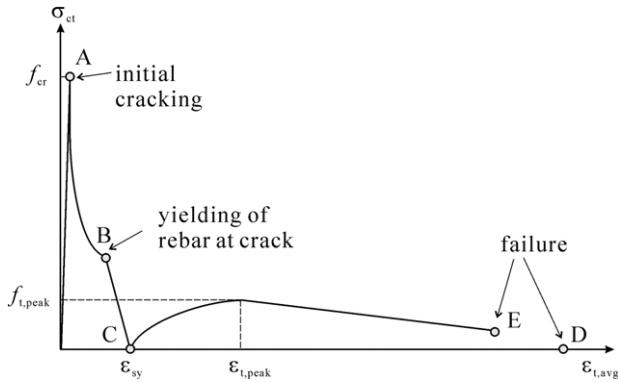


Fig. 8. Variation of average tensile stress in concrete up to failure.

effect on the average strain of reinforced concrete at the peak tensile stress of concrete after yielding of reinforcement, as presented in Fig. 11. Hence, with the concrete compressive strength and yield strength of reinforcement fixed at 40 MPa and 400 MPa, respectively, the effects of the reinforcement hardening strain, strain hardening modulus, bar diameter and reinforcement ratio were investigated.

Fig. 12 shows the relationship between bar diameter and average tensile strain at the peak tensile stress of concrete for a range of hardening strains, averaged for the various reinforcement ratios and strain hardening moduli considered. As shown in this figure, the average strain of reinforced concrete at the peak stress is significantly affected by the hardening strain of the reinforcement. On the other hand, the average strain at the peak stress is only slightly affected by hardening modulus of the reinforcement except for the case of a relatively small hardening strain. This result can also be deduced from Figs. 1 and 5 since the stress difference between line C–E and line C–D in Fig. 1 is largest near the hardening strain of reinforcement. With the minimum value presented in Fig. 12, the average strain at peak tensile stress of concrete can be simply expressed as follows:

$$\varepsilon_{t,peak} = 0.01 + 0.001 \cdot \max(15 - d_b, 0) \geq \varepsilon_{sh}. \quad (11)$$

#### 4.4. Tension stiffening model after yielding of reinforcement

For the pre-peak behavior after yielding of reinforcement, the concrete average tensile stress–strain relationship can be simply assumed to be parabolic in nature, as suggested by the analysis results shown in Figs. 6 and 7. On the other hand, for the post-peak behavior, the average tensile stress of concrete after yielding of reinforcement converges to the value of  $f_{ct,peak}$  for  $\rho_{min}$  (0.54% in Fig. 7). In this paper, the reinforcement ratio which causes the reinforcement to yield upon initial cracking is used for  $\rho_{min}$ . In the post-yield tension stiffening model proposed, the post-peak stress behavior of concrete is assumed to be such that the average tensile stress linearly decreases with increasing average tensile strain, and that the average tensile stress is constant as  $f_{ct,peak}$  for  $\rho_{min}$  for average strains larger than 0.1.

Consequently, the proposed average tensile stress–strain relationship of concrete, after yielding of the reinforcement, is as follows:

$$f_{ct,avg} = f_{ct,peak} - f_{ct,peak} \left( \frac{\varepsilon_{t,peak} - \varepsilon_{t,avg}}{\varepsilon_{t,peak} - \varepsilon_{sy}} \right)^2 \quad \text{for } \varepsilon_{sy} \leq \varepsilon_{t,avg} \leq \varepsilon_{t,peak} \quad (12a)$$

$$f_{ct,avg} = f_{ct,peak} - \frac{f_{ct,peak} - 0.5f_{ct,peak,\rho_{min}}}{0.1 - \varepsilon_{t,peak}} (\varepsilon_{t,avg} - \varepsilon_{t,peak}) \geq 0.5f_{ct,peak,\rho_{min}} \quad \text{for } \varepsilon_{t,avg} \geq \varepsilon_{t,peak} \quad (12b)$$

where  $\rho_{min} = (\varepsilon_{cr} \cdot E_c) / (f_{sy} - \varepsilon_{cr} \cdot E_s)$ .

of reinforcement was highly affected by concrete compressive strength, diameter of reinforcement, and reinforcement ratio; it was only slightly affected by the yield strength, hardening behavior of the reinforcement, as presented in Fig. 9. Since the bond strength and tensile strength of concrete are proportional to the square root of the compressive strength, it will be assumed that the peak stress in concrete after yielding of reinforcement can be modeled by the following expression:

$$f_{ct,peak} = a\sqrt{f'_c}. \quad (9)$$

In this equation, the coefficient  $a$  represents the effects of reinforcement diameter and reinforcement ratio, both found to be significant parameters. Fig. 10 shows the variation of the coefficient  $a$  for a range of reinforcement diameters and ratios. In this plot, the value of  $a$  was averaged for a range of reinforcement yield strengths and concrete compressive strengths, both of which were found to have little influence. It was found that the relationship between coefficient  $a$  and the reinforcement diameter and ratio can be approximated by the following relationship:

$$a = -0.0313\rho_s^{0.57}d_b + 3.3881\rho_s^{0.76}. \quad (10)$$

Note from Eqs. (9) and (10) that the peak stress of concrete after yielding of reinforcement increases with increasing longitudinal reinforcement ratio and with decreasing reinforcement diameter. This is consistent with well-known aspects of the tension stiffening phenomenon; that is, higher longitudinal reinforcement ratios and smaller reinforcement diameters result in greater tensile stress being transferred to the concrete.

#### 4.3. Strain at the peak average tensile stress of concrete

Parametric analyses revealed that the concrete compressive strength and yield strength of reinforcement have only a marginal

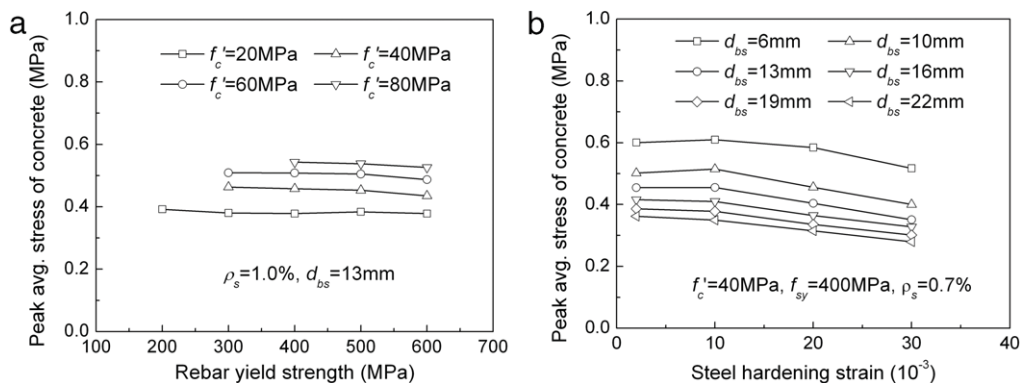


Fig. 9. Effect of (a) yield strength; and (b) hardening strain of the rebar on the peak tensile stress after yielding of reinforcement.

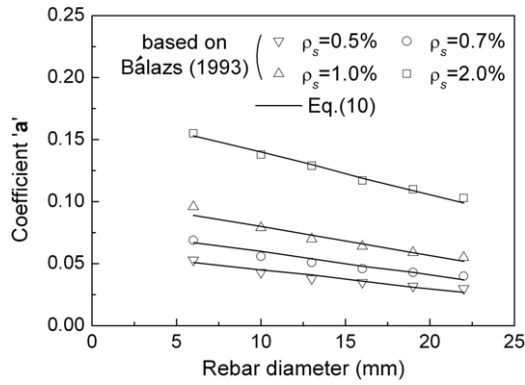


Fig. 10. Variation of the coefficient 'a'.

#### 4.5. Average tensile strain of reinforced concrete causing rupture of reinforcement

With the proposed tension stiffening model, the steel stress at a crack can be more precisely calculated from the force equilibrium condition at the crack according to the following equation:

$$f_{scr} = f_{s,avg} + f_{ct,avg}/\rho_s \quad (13)$$

As mentioned previously, the average tensile strain of reinforced concrete which causes rupture of an embedded rebar is significantly less than the rupture strain of the bare bar since the average concrete tensile stress is not zero even after yielding of reinforcement (see Fig. 1). Satisfying the equilibrium at a crack as described by Eq. (13), under the assumption that steel stress–strain relationship after hardening strain ( $\epsilon_{sh}$ ) is linear, the average tensile strain of reinforced concrete at the reinforcement rupture can be derived from Eq. (12b). Thus:

$$\epsilon_{t,avg,rupt} = \frac{B - \sqrt{B^2 - 4AC}}{2A} \quad (14a)$$

for  $f_{su} \leq f_{scr,\epsilon_{t,peak}}$

$$\epsilon_{t,avg,rupt} = \frac{\epsilon_{sh}E_{sh} + f_{su} - f_{sy} - \frac{0.5f_{ct,peak,\rho_{min}}}{\rho_s} - \epsilon_{t,peak}K_E}{E_{sh} - K_E} \quad (14b)$$

for  $f_{scr,\epsilon_{t,peak}} \leq f_{su} \leq f_{scr,0.1}$

$$\epsilon_{t,avg,rupt} = \epsilon_{sh} + \frac{1}{E_{sh}} \left( f_{su} - f_{sy} - \frac{0.5f_{ct,peak,\rho_{min}}}{\rho_s} \right) \quad (14c)$$

for  $f_{scr,0.1} \leq f_{su}$

where,  $A = \frac{f_{ct,peak}}{(\epsilon_{t,peak} - \epsilon_{sy})^2}$ ,  $B = \rho_s E_{sh} + 2A\epsilon_{t,peak}$ ,

$C = \rho_s (f_{su} - f_{sy} + E_{sh}\epsilon_{sh}) - f_{ct,peak} + A\epsilon_{t,peak}^2$ ,

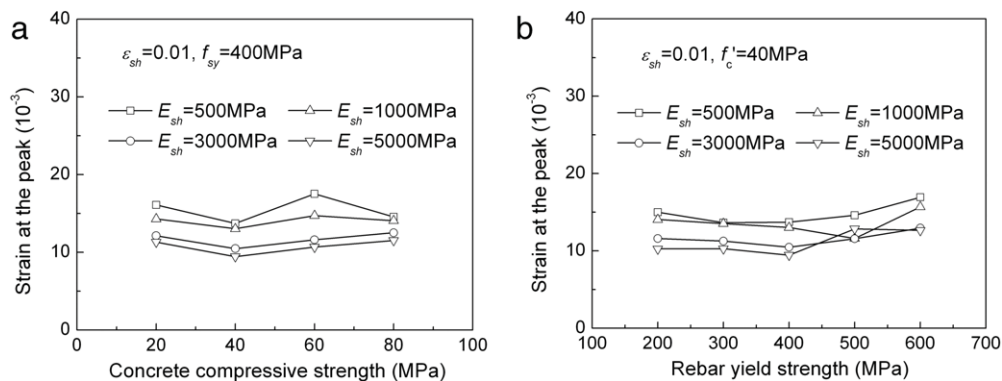


Fig. 11. Effect of (a) concrete compressive strength; and (b) rebar yield strength on the average strain at peak tensile stress after yielding of reinforcement.

$$f_{scr,0.1} = f_{sy} + (0.1 - \epsilon_{sh}) E_{sh} + \frac{0.5f_{ct,peak,\rho_{min}}}{\rho_s},$$

$$K_E = \frac{1}{\rho_s} \frac{f_{ct,peak} - 0.5f_{ct,peak,\rho_{min}}}{0.1 - \epsilon_{t,peak}}$$

Fig. 13 shows the variation of average tensile strain of reinforced concrete causing the rupture of reinforcement predicted by the above formulation. This figure indicates that the average tensile strain of reinforced concrete at the rupture of reinforcement with small rebar diameter, small reinforcement ratio, and high compressive strength of concrete is significantly lower than the rupture strain of the reinforcement. This tendency is consistent with typically observed behavior in that the average tensile stress of concrete increases with small rebar diameter due to an increased bond efficiency, and that concrete contribution to tensile stress becomes significant in elements with low reinforcement ratios and/or high concrete compressive strengths.

## 5. Model verification

### 5.1. Uniaxial tensile behavior of RC members

For verification of the proposed model, the uniaxial tension members tested by Mayer and Elgehausen [14] were studied. To facilitate normalized comparisons, the ratio of the average tensile strain of reinforced concrete to the steel strain at a crack ratio ( $\epsilon_{t,avg}/\epsilon_{scr}$ ) was employed. A higher value of the ratio indicates a lower average tensile stress in concrete.

As shown in Fig. 14, the model proposed in this study (Eq. (12)) shows good agreement with the experimental results, while CEB-FIP MC90 [3] cannot predict the actual concrete contribution to the tensile behavior after yielding of reinforcement. The CEB formulation is deficient because the steel stress at a crack is not checked against the reinforcement's yield strength limit.

Fig. 15 shows results relating to the average member strain at the ultimate state, governed by bar rupture. In this figure, the bare bar response also represents the response obtained from the tension stiffening models proposed by several researchers [4–8] since no considered is given, in these models, to the concrete tensile stress contribution after yielding of reinforcement. As is evident from Fig. 15 and Table 2, the bare bar response significantly overestimates the deformation capacity of reinforced concrete tension members. The results obtained from MC90 are also widely scattered. The proposed model provides improved predictions of the average tensile strain at ultimate with a mean ratio value of 0.945 and a standard deviation of 0.285.

### 5.2. Flexural behavior of reinforced concrete beams

Since the proposed model considers the average tensile stresses in concrete after yielding of the reinforcement, the flexural

**Table 2**  
Comparison of ultimate strains for uniaxial tensile specimens.

Specimen	Ultimate strain				Ratio		
	Test (1)	Bare bar (2)	MC90 (3)	Proposed (4)	(2)/(1)	(3)/(1)	(4)/(1)
S8D6-B	0.0041	0.0306	0.0157	0.0061	7.431	3.813	1.476
S4D12-B	0.0051	0.0330	0.0131	0.0060	6.453	2.557	1.179
S16D6-S	0.0943	0.1650	0.0782	0.0939	1.749	0.829	0.995
S8D12-A	0.0393	0.0740	0.0462	0.0297	1.881	1.176	0.754
S8D16-A	0.0463	0.0875	0.0517	0.0326	1.888	1.117	0.703
S4D25-A	0.0658	0.0954	0.0621	0.0493	1.449	0.944	0.748
S4D12-A	0.0220	0.0740	0.0267	0.0267	3.367	1.217	1.214
S4D16-A	0.0457	0.0875	0.0279	0.0310	1.914	0.610	0.677
S2D25-A	0.0652	0.0954	0.0433	0.0495	1.462	0.663	0.759
				Mean	3.066	1.436	0.945
				Standard deviation	2.282	1.061	0.285

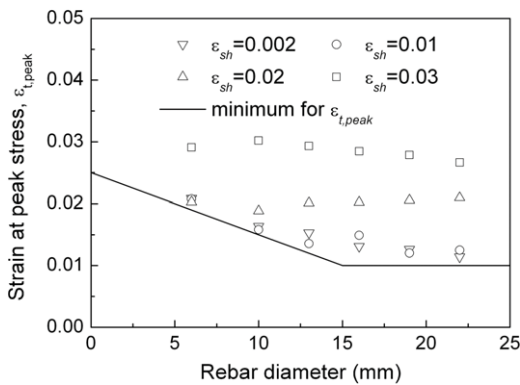


Fig. 12. Average strain at peak tensile stress after yielding of reinforcement.

ductility of reinforced concrete beams, especially with respect to rupture of the reinforcement, can presumably be more accurately predicted. To investigate the effect of the proposed model on flexural ductility, a rectangular section of 600 × 900 mm reinforced with one layer of tension reinforcement was considered. In this example, the concrete compressive strength and the reinforcement yield strength were fixed at 60 MPa and 400 MPa, respectively. The stress–strain relationship of the reinforcement was assumed as tri-linear with  $\epsilon_{sh} = 0.015$  and  $E_{sh} = 1500$  MPa. The ultimate strengths of 500 and 600 MPa were considered with the rupture strains of 0.082 and 0.148 for the reinforcement, respectively.

A layered sectional analysis was performed for the condition of pure bending. The reinforcement was assumed to be smeared in a tributary area of 7.5 times the bar diameter as suggested by CEB-FIP MC90 [3]. A parabolic stress–strain relationship [15] was used for the concrete compressive behavior as shown in Fig. 16, while the tension stiffening model presented by Vecchio and Collins [6] was used for the concrete tensile behavior when

the average tensile strain of the concrete, at the level of the reinforcement, was less than the yield strain of reinforcement. The force equilibrium at a crack was checked, so the average tensile stress of concrete was limited by the yielding of reinforcement at a crack. After the average tensile strain exceeded the yield strain of the reinforcement, the average tensile stress of concrete was calculated using Eq. (12), developed in this study. It should be noted that the selection of the tension stiffening model before yielding did not affect the response after yielding.

Fig. 17 shows that when the tensile reinforcement ruptures before concrete crushing, the flexural ductility predicted by the proposed model is notably less than that obtained ignoring post-yield tension stiffening effects. Comparing  $f_{su} = 500$  MPa and  $f_{su} = 600$  MPa, it can be seen that the average tensile stress of concrete after yielding of reinforcement should be considered especially in flexural members with reinforcement for which the difference between the rupture strength and the yield strength is relatively small.

### 5.3. Shear behavior of RC beams

In reinforced concrete beams subjected to shear forces, tension stiffening effects after yielding of reinforcement can be significant since stirrups are likely to rupture earlier than the longitudinal reinforcement, particularly in beams containing low amounts of shear reinforcement. Eq. (14) and the previous analysis results for tension members suggest that the average tensile strain causing rupture of a stirrup is significantly less than the ultimate strain of the bare bar, particularly when the difference between the rupture strength and the yield strength is small.

To investigate this influence, the proposed tension stiffening model was implemented in VecTor2 [1], a 2D nonlinear finite element analysis program based on the Disturbed Stress Field Model (DSFM) [17,18]. Specimens B3 and C3, shear-critical beams tested by Vecchio and Shim [19] were analyzed for

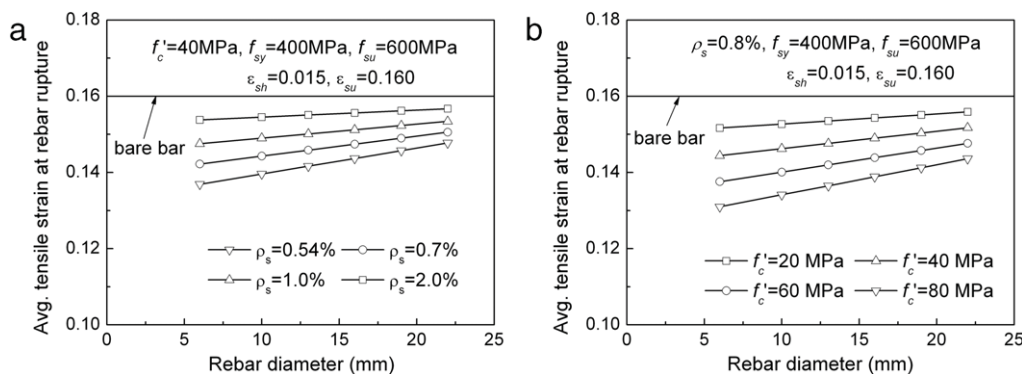


Fig. 13. Variation of average tensile strain at rebar rupture; (a) effect of longitudinal reinforcement ratio; (b) effect of concrete compressive strength.

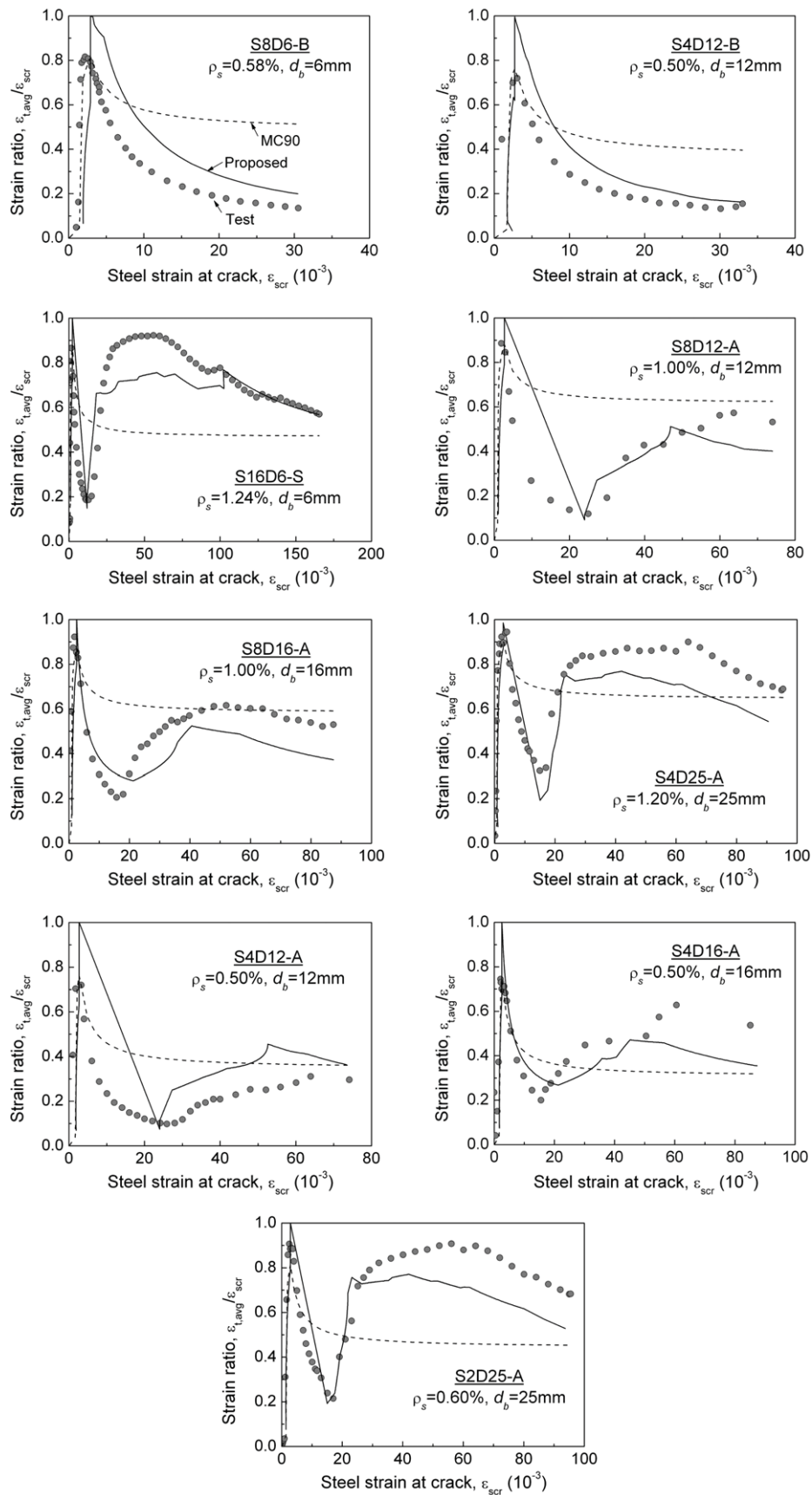


Fig. 14. Comparison with test results of members subjected to uniaxial tension.

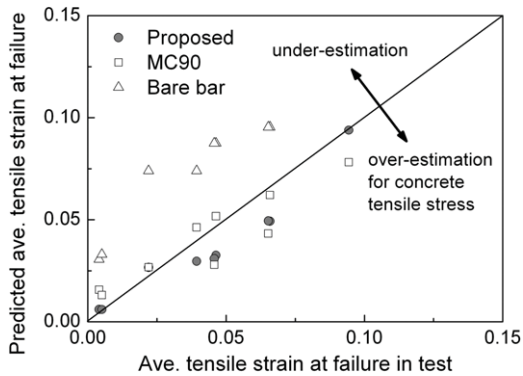


Fig. 15. Comparison of ultimate strains for uniaxial tensile specimens.

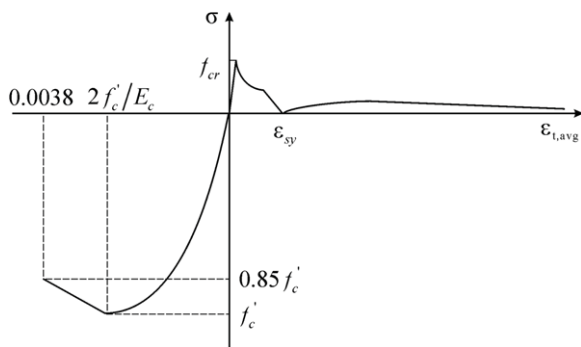


Fig. 16. Stress-strain relationship of concrete [6,16].

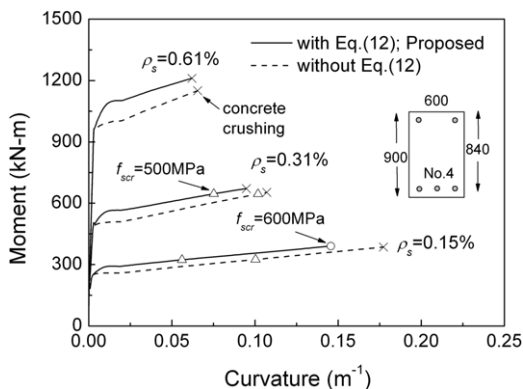


Fig. 17. Moment-curvature capacity of reinforced concrete beams.

illustrative purposes. Specimens B3 and C3 contained 2.96% and 3.46% longitudinal reinforcement, and 0.15% and 0.20% shear reinforcement, respectively. The concrete compressive strength

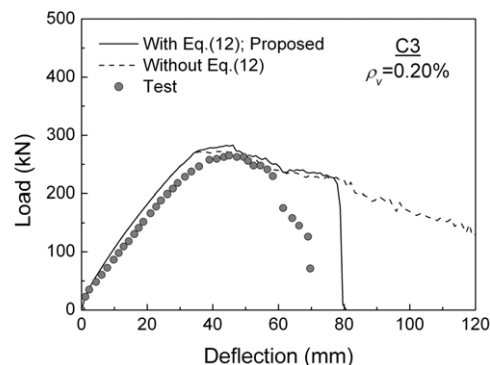
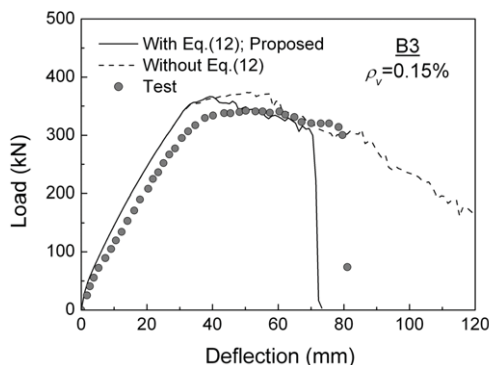


Fig. 18. Analysis results for shear-critical beams.

was 43.5 MPa, and the yield strength and ultimate strength of the stirrups were 600 MPa and 650 MPa, respectively. The longitudinal reinforcement was modeled with truss elements, the stirrups were represented as smeared reinforcement, and the concrete section was modeled with 4-node rectangular elements, using the same mesh layouts as described in Vecchio and Shim [19].

The analysis results obtained are compared with the experimental results in Fig. 18. While the analysis results are almost identical for the pre-peak behavior, the proposed model predicts that the stirrups in the vicinity of the tensile longitudinal reinforcement rupture due to the effect of the average concrete tensile stress after yielding. The resulting reduced ductility in the load-deflection responses better matches the experimentally observed behavior. Thus, for shear-critical members potentially governed by rupture of the stirrup steel, the effects of tension stiffening after yielding of reinforcement can have a major influence on the computed shear ductility.

## 6. Concluding remarks

The contribution of concrete tension stiffening effects to the post-yielding deformation response of reinforced concrete members was investigated, and a simplified constitutive model was formulated. In developing the model, a crack analysis procedure taking into account the bond slip-stress relationship between concrete and reinforcement was employed. Findings and conclusions derived from this study are summarized as follows:

1. Using the crack analysis procedure described by Balázs [11], analyses were made of reinforced concrete members subjected to uniaxial tension with particular focus on the post-yielding behavior. It was shown that significant average tensile stresses still exist in concrete even after yielding of reinforcement, contrary to what has been typically assumed. The analysis results showed good agreement with experimental results.
2. To derive a post-yield tension stiffening model for unconfined concrete members with good bond, an analytical parametric study was conducted with the main variables being the material properties of the concrete and reinforcement steel. The parametric analysis results showed that the average tensile stress in concrete increases from zero at the point of yielding of the reinforcement, peaks, and then gradually diminishes. A simplified constitutive model was formulated accordingly, with concrete compressive strength, rebar diameter and reinforcement ratio being the main influencing parameters.
3. The average tensile strain of a reinforced concrete member which results in rupture of the reinforcement can be significantly less than that causing rupture of the bare bar. The proposed model considers this effect, and thus it can be useful for evaluating of the ductility of reinforced concrete members.

4. The behavior predicted by the proposed tension stiffening model was compared to experimental results from members subjected to uniaxial tension. The proposed model was found to predict, reasonably accurately, the variation of average tensile stresses in the concrete as well as the average tensile strain at failure.
5. The influence of post-yield tension stiffening effects on the behavior of flexural members was investigated. Analysis results showed that the curvature at ultimate can be decreased when the tensile reinforcement ruptures before concrete crushing in the compression zone; this occurs only in members with low flexural reinforcement ratios and low reinforcement yield-to-ultimate strength ratios. Otherwise, the influence is minimal.
6. The analysis model was implemented into a nonlinear finite element program and applied to the analysis of beams in shear. The influence of post-yield tension stiffening on the ductility of shear-critical beams was shown to be significant, particularly for beams having low shear reinforcement ratios. The analysis results obtained with the proposed model gave improved predictions for shear ductility and rupture of stirrups.

### Acknowledgements

This research was partly supported by the Seoul National University, Integrated Research Institute of Construction and Environmental Engineering.

### References

- [1] Wong PS, Vecchio FJ. VecTor2 & formworks user's manual. Publication no. 2002-02. Toronto (ON, Canada): Department of Civil Engineering, University of Toronto; 2002.
- [2] Bentz EC. Sectional analysis of reinforced concrete members. Doctorate thesis. Toronto (ON, Canada): Department of Civil Engineering, University of Toronto; 2000.
- [3] Comité Euro-international du Béton-Federation internationale. CEB-FIP model code for concrete structures. London: Thomas Telford; 1990.
- [4] Vecchio FJ, Collins MP. Response of reinforced concrete to in-plane shear and normal stresses. Publ. no. 82-03. Toronto (ON, Canada): Department of Civil Engineering, University of Toronto; 1982.
- [5] Collins MP, Mitchell D. Prestressed concrete basics. Ottawa (ON, Canada): Canadian Prestressed Concrete Institute; 1987.
- [6] Vecchio FJ, Collins MP. The modified compression field theory for reinforced concrete elements subjected to shear. *ACI J Proc* 1986;83(6):219–31.
- [7] Bentz EC. Explaining the riddle of tension stiffening models for shear panel experiments. *J Struct Eng, ASCE* 2005;131(9):1422–5.
- [8] Stramandinoli RSB, Rovere HLL. An efficient tension-stiffening model for nonlinear analysis of reinforced concrete members. *Eng Struct* 2008;30:2069–80.
- [9] Kaklauskas G, Gribniak V, Bacinskas D, Vainiunas P. Shrinkage influence on tension stiffening in concrete members. *Eng Struct* 2009;31:1305–12.
- [10] Wu HQ, Gilbert RI. Modeling short-term tension stiffening in reinforced concrete prisms using continuum-based finite element model. *Eng Struct* 2009;31:2380–91.
- [11] Balázs GL. Cracking analysis based on slip and bond stresses. *ACI Mater J* 1993;90(4):320–48.
- [12] Oh BH, Kim SH. Advanced crack width analysis of reinforced concrete beams under repeated loads. *J Struct Eng, ASCE* 2007;133(3):411–20.
- [13] Ruiz MF, Muttoni A, Gambarova PG. Analytical modeling of the pre- and postyield behavior of bond in reinforced concrete. *J Struct Eng, ASCE* 2007;133(10):1364–72.
- [14] Mayer U, Eligehausen R. Bond behavior of ribbed bars at inelastic steel strains. In: 2nd Int. Ph.D. symposium in civil engineering. 1998. p. 1–8.
- [15] CSA Standard A23.3, A23.3-04. Design of concrete structures. Mississauga (ON, Canada): Canadian Standards Association; 2004.
- [16] Park R, Pauley T. Reinforced concrete structures. New York: John Wiley & Sons; 1975.
- [17] Vecchio FJ. Disturbed stress field model for reinforced concrete: formulation. *J Struct Eng, ASCE* 2000;126(9):1070–7.
- [18] Vecchio FJ. Disturbed stress field model for reinforced concrete: implementation. *J Struct Eng, ASCE* 2001;127(1):12–20.
- [19] Vecchio FJ, Shim W. Experimental and analytical reexamination of classic concrete beam tests. *J Struct Eng, ASCE* 2004;130(3):460–9.